Mechanism of the Kolbe−Schmitt Reaction. Structure of the Intermediate Potassium Phenoxide−CO_2 Complex

Zoran Marković,[†] Svetlana Marković,*[,‡] Nedeljko Manojlović,[§] and Jasmina Predojević-Simović[†]

Faculty of Agronomy, University of Kragujevac, 34 Cara Dušana, 32000 Čačak, Serbia, Faculty of Science, University of Kragujevac, 12 Radoja Domanovića, 34000 Kragujevac, Serbia, and Faculty of Medicine, University of Kragujevac, 69 Svetozara Markovića, 34000 Kragujevac, Serbia

Received February 19, 2007

Our investigation elucidates the structure of the intermediate in the first stage of the carboxylation reaction of potassium phenoxide. Under the reduced pressure of carbon dioxide the complex is not solvated with the CO_2 molecules. Under the conditions of the carboxylation reaction the potassium phenoxide−carbon dioxide complex is solvated with one or two CO_2 molecules. One of the added CO_2 moieties performs an electrophilic attack on the benzene ring, whereas the old CO_2 moiety becomes a molecule of solvent. Our findings are in good accord with the experimental results obtained by the NMR and IR measurements.

INTRODUCTION

A carboxylation reaction of alkali metal phenoxides with carbon dioxide, where hydroxybenzoic acids are formed, is called the Kolbe−Schmitt reaction. The carboxylation reaction of potassium phenoxide (Figure 1) was performed at different temperatures and pressures (20−240 °C and 5−40 MPa).[1−4] It was observed that the yield of the reaction and distribution of products were highly dependent on the experimental conditions.

The mechanism of the Kolbe−Schmitt reaction has been the subject of numerous experimental and theoretical investigations. Early researchers supposed that the reaction proceeded via an intermediate alkali metal phenyl carbonate ($PhO-CO_2Na$).[1−3] This idea was supported by Daives[5] and Ayres,[6] and the evidence of the formation of a weak chelate complex between sodium phenoxide and carbon dioxide was found by means of infrared absorption spectra.[7] On the basis of FT-IR spectra and DTA analysis the presence of the intermediate $NaOPh-CO_2$ complex was confirmed by Kunert.[8] It was also found that the complex changed to a further intermediate at increased temperature (75−80 °C). It was concluded that a direct carboxylation could be excluded from the Kolbe−Schmitt reaction mechanism. Achenie, Stanescu,[9,10] and the authors of this paper[11,12] proposed a mechanism including the initial formation of the $MOPh-CO_2$ complex (M stands for an alkali metal).[13] They showed that carbon dioxide needed to be activated to build hydroxybenzoic acids with alkali metal phenoxide. This activation was realized by coordinating carbon dioxide to the alkali metal.[9−12] In this way the $MOPh-CO_2$ complex was formed. As the carboxylation reaction further occurred, a direct carboxylation of the benzene ring with another molecule of carbon dioxide did not take place. Instead, the CO_2 moiety of the $MOPh-CO_2$ complex performed an electrophilic attack on the benzene ring in the ortho and para positions, forming the intermediates oC and pC via the oTS1 and pTS1 transition states. The first and second stages of the carboxylation reaction of potassium phenoxide[12] are presented in Figure 2. It was shown that the intramolecular conversion of the $MOPh-CO_2$ complex was the most responsible for the products distribution of the Kolbe−Schmitt reaction. It was observed that the mechanism of the carboxylation reaction of lithium phenoxide was significantly different from those of other alkali metal phenoxides,[12] and that there was a significant resemblance between the mechanisms of the carboxylation reactions of lithium and sodium phenoxides.[11,12] For this reason the mechanism of the Kolbe−Schmitt reaction of lithium and sodium phenoxides was reinvestigated using the B3LYP/CEP-31+G(d) method.[14] The results of this investigation were in perfect agreement with the findings obtained by means of the B3LYP/LANL2DZ method. It was concluded that the introduction of polarization and diffusion functions did not affect the outcome of the calculations and that the deviation of lithium and sodium phenoxides from the mechanisms of carboxylations of other alkali metal phenoxides was a consequence of short ionic radii of lithium and sodium.

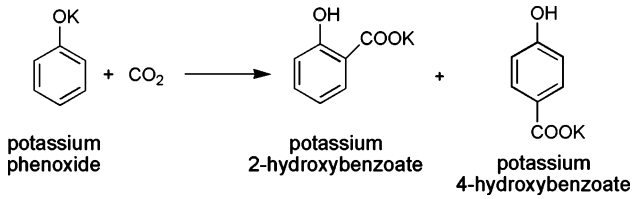

Figure 1. General outline of the carboxylation reaction of potassium phenoxide.

On the other hand, there are opposite discussions concerning the Kolbe−Schmitt reaction mechanism. Among several postulations[3,4,15,16] a mechanism including a direct carboxylation of the benzene ring is worth mentioning. Kosugi et al.[4] investigated the Kolbe−Schmitt reaction mechanism of phenol and 2-naphthol. It was concluded that a direct

* Corresponding author e-mail: mark@kg.ac.yu.
[†] Faculty of Agronomy.
[‡] Faculty of Science.
[§] Faculty of Medicine.

10.1021/ci700068b CCC: $37.00
Published on Web 05/19/2007

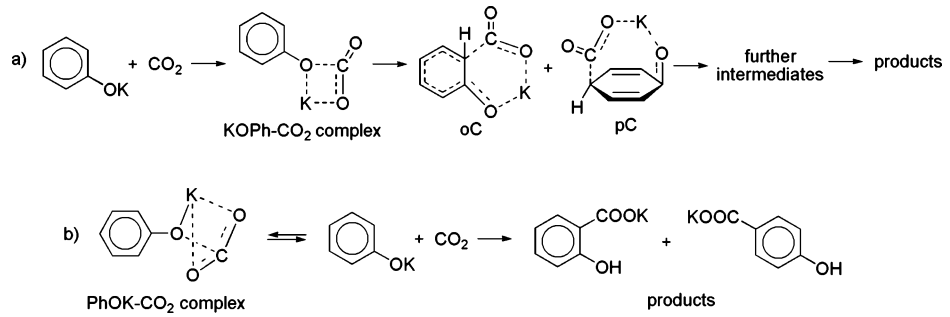

Figure 2. (a) Intermediates in the first and second stages of the carboxylation reaction of potassium phenoxide proposed in ref 12. (b) Mechanism of direct carboxylation proposed by Kosugi et al.[4] and competitive formation of the PhOK−CO_2 complex (structure A).

carboxylation of phenoxide with carbon dioxide took place and was competitive with the formation of the KOPh−CO_2 (or NaOPh−CO_2) complex (Figure 2). It should be pointed out that Kosugi et al. prepared a "pure potassium phenoxide−carbon dioxide complex" by introducing CO_2 of 0.1 MPa onto fine powdered phenoxide for 24 h. The CP-MAS NMR spectrum of the CO_2 complex enriched with carbon-13 showed a peak at 154 ppm. Experiments using a carbon-13 labeled complex led to the following conclusions: the CO_2 complex prepared with carbon dioxide enriched with carbon-13 did not yield carboxylic acids with labeled carbon-13 but scrambled with "normal" carbon dioxide. On the basis of C-13 NMR and MOPAC/PM3 calculations a carbonate-like complex (PhOK−CO_2) was proposed for the intermediate of the Kolbe−Schmitt reaction.[4] The structure of this complex is presented in Figure 2 (structure A).

It turns out that, in spite of numerous investigations, the structure of the intermediate formed in the first stage of the Kolbe−Schmitt reaction has not been elucidated. This is probably the consequence of the very hygroscopic nature of the complex and its contamination with inorganic carbonates. In this work we present solid evidence that the KOPh−CO_2 complex is the intermediate in the first stage of the carboxylation reaction of potassium phenoxide.

COMPUTATIONAL METHODS

Geometrical parameters of all stationary points and transition states for the reaction of potassium phenoxide and carbon dioxide are optimized in vacuum, employing analytic energy gradients by means of the Becke-type three-parameter hybrid combined with the gradient-corrected correlation functional of Lee, Yang, and Parr.[17,18] This functional, commonly known as B3LYP,[17−19] implemented in the GAUSSIAN98 program package,[20] turned out to be quite reliable for geometrical optimizations.[21] All theoretical calculations are carried out by employing the LANL2DZ[22−24] basis set, because it proved to be reliable and reproducible for the investigations of the Kolbe−Schmitt reaction mechanism.[9−12] The first row atoms are described by the double-ζ basis Dunning-Hay.[25] The LANL2DZ basis set also includes effective core potentials used to include some relativistic effects for potassium.

To describe solvent effects to the structure and energy of the first intermediate in the carboxylation reaction of potassium phenoxide the microsolvated model is used, since continuum-based models are not suitable for modeling chemical reactions involving gaseous species. Solvent is simulated by adding one and two discrete carbon dioxide molecules.

The vibrational analysis and the natural bond orbital (NBO) analysis[26] are performed for all structures at the B3LYP/LANL2DZ level. All the fully optimized transition state structures are confirmed by the existence of a sole imaginary frequency, whereas the optimized intermediate structures possess only real frequencies. From the transition structures, the intrinsic reaction coordinates (IRCs) are obtained using the IRC routine in Gaussian 98.

RESULTS AND DISCUSSION

Note that Kosugi et al. prepared the complex at the pressure of carbon dioxide of 0.1 MPa at room temperature.[4] These conditions are far below the temperature and pressure of carbon dioxide needed to yield hydroxybenzoic acids in the Kolbe−Schmitt reaction[1−3] and are suitable for keeping the potassium phenoxide−carbon dioxide complex. We assume that, under these conditions, the potassium phenoxide−carbon dioxide complex is not solvated by other molecules of CO_2. The first part of our investigation is devoted to the structure and properties of the potassium phenoxide−carbon dioxide complex.

Since the carboxylation reaction is performed in a large excess of carbon dioxide, it is reasonable to expect that carbon dioxide behaves as a solvent, implying that more than one CO_2 molecule can be coordinated to the alkali metal. The second part of our investigation is devoted to the influence of carbon dioxide as solvent upon the structure and energy of the intermediate potassium phenoxide−carbon dioxide complex. Thus, we investigate the following processes that can represent the first step of the carboxylation reaction of potassium phenoxide

$$\text{Model } n = 0:\ \text{PhOK} + \text{CO}_2 \rightarrow \text{KOPhCO}_2 \quad (\text{B}_0) \quad (1)$$

$$\text{Model } n = 1:\ \text{KOPhCO}_2 + \text{CO}_2 \rightarrow \text{KOPh(CO}_2)_2 \quad (\text{B}_1) \quad (2)$$

$$\text{Model } n = 2:\ \text{KOPh(CO}_2)_2 + \text{CO}_2 \rightarrow \text{KOPh(CO}_2)_3 \quad (\text{B}_2) \quad (3)$$

where B_n represents the potassium phenoxide−carbon dioxide complex solvated with n molecules of CO_2.

It has been shown that the intramolecular conversion of the alkali metal phenoxide−carbon dioxide complex is the most responsible for the products distribution in the Kolbe−Schmitt reaction.[8−12,14] For this reason the conversions of the potassium phenoxide−carbon dioxide complex and solvated complexes to further intermediates are also examined in this work. The second step of the carboxylation

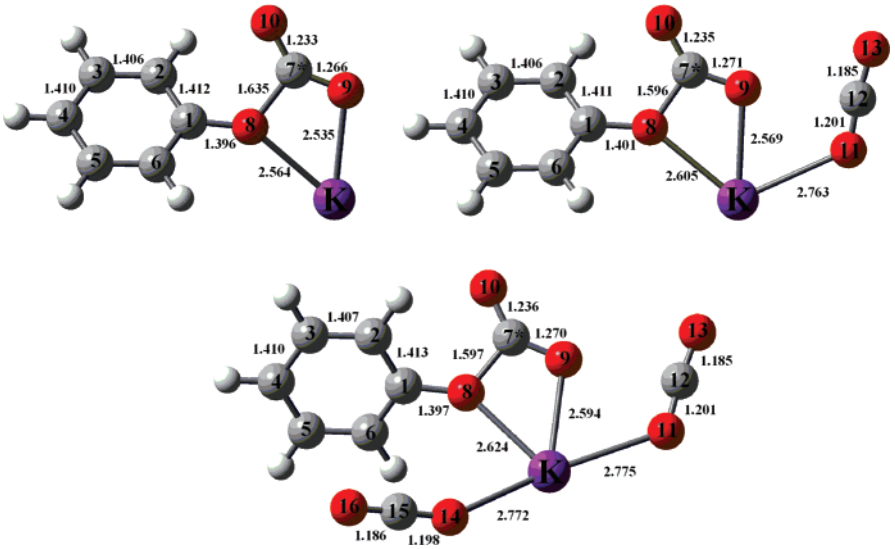

Figure 3. Optimized geometries of the intermediates B_0 (top left), B_1 (top right), and B_2 (bottom) with selected bond lengths in Å. B_0 stands for the KOPh−CO_2 complex, whereas B_1 and B_2 denote the complexes solvated with one and two CO_2 molecules, respectively. Dark gray and red balls represent carbon and oxygen atoms, respectively.

reaction of potassium phenoxide can be presented with the following equations

$$\text{Model } n = 0:\ B_0 \rightarrow oC_0 + pC_0 \quad (4)$$

$$\text{Model } n = 1:\ B_1 \rightarrow oC_1 + pC_1 \quad (5)$$

$$\text{Model } n = 2:\ B_2 \rightarrow oC_2 + pC_2 \quad (6)$$

where C_n denotes the second intermediate solvated with n molecules of CO_2, and the prefixes o and p stand for the ortho and para routes of the Kolbe−Schmitt reaction. It should be noted that the reactions 1 and 4 were investigated in ref 12.

We assume that the model $n = 0$ is applicable under the low pressure of CO_2, whereas models $n = 1$ and $n = 2$ are applicable under the enhanced pressure of CO_2.

STRUCTURE OF THE POTASSIUM PHENOXIDE−CARBON DIOXIDE COMPLEX

Equation 1 is simulated by approaching the reactants to each other. The KOPh−CO_2 complex (intermediate B_0) is formed, and its optimized geometry is presented in Figure 3. The carbon atom belonging to the CO_2 moiety of B_0 is marked by an asterisk. This marked intermediate B_0 is analogous to the potassium phenoxide−carbon dioxide complex prepared by Kosugi et al. using $^{13}CO_2$.

Structure B_0, proposed in this paper (Figure 3), is obviously different from structure A (Figure 2), suggested by Kosugi et al. The difference in the structure of the intermediate in the first stage of the carboxylation reaction of PhOK can be a consequence of the level of theory used in the work of Kosugi et al. to predict structure A (semiempirical PM3 method).[4] On the other hand, structure B_0 is in agreement with Kosugi's experimental results. Our results complement and explain the experiments of Kosugi et al. This matter will be presented in the text that follows.

The carbon-13 NMR properties of the KOPh−CO_2 complex are predicted, and the relative shifts for all carbon atoms relative to TMS are calculated. Since the complex belongs to the C_1 point group, ortho and meta carbons show two different values for chemical shift in the NMR spectrum. In this case the corresponding mean values are taken to represent the chemical shifts of the ortho and meta carbons. Thus, the chemical shifts of the carboxyl, ortho, meta, and para carbons are as follows: 152, 119, 126, and 118 ppm, respectively. Note that the experimental values for the same carbon atoms of the potassium phenoxide−carbon dioxide complex are as follows: 154, 121.4, 130.4, and 115 ppm, respectively.[4]

The vibrational analysis of the KOPh−CO_2 complex is performed. There is a strong vibration of the CO_2 moiety at 1842 cm^{-1}. This value is significantly different from the experimental value of 1650 cm^{-1}.[4] There is a similar situation with the NaOPh−CO_2 complex, whose experimental vibrational frequency of the CO_2 moiety amounts to 1685 cm^{-1},[7,8] whereas the computed value equals 1868 cm^{-1}. It is well-known that the computed values of vibrational frequencies contain a systematic error due to the neglect of electron correlation. There is also a contribution to the error due to the fact that the calculated frequencies come from treating the potential energy surface near the stationary point as a harmonic oscillator. In reality, the potential energy surface near the stationary point is generally anharmonic. This results in overestimating the vibrational frequencies values, on average, by anywhere between 0 and 20%, implying that they need to be scaled to provide satisfactory approximation of experimental vibrational frequencies. By applying a scaling factor for B3LYP/LANL2DZ of 0.961 ± 0.079[27] to the computed values of vibrational frequencies for KOPh−CO_2 and NaOPh−CO_2 complexes, the agreement with experimental data is improved.

Such agreement between experimental and theoretical results indicates that the structure of the potassium phenoxide−carbon dioxide complex used for experimental NMR and IR measurements[4] corresponds to that of the intermediate B_0 (Figure 3). In other words, B_0 represents the structure of the potassium phenoxide−carbon dioxide complex under the reduced pressure of carbon dioxide.

Table 1. Relative Free Energies of the Species Involved in the First and Second Steps of the Carboxylation Reaction of Potassium Phenoxide[a]

G^{298} (kcal/mol)	B_n	$oTS1_n$	$pTS1_n$	oC_n	pC_n	ortho/para ratio (%)
$n = 0$	−10.88	4.80	6.36	4.55	6.07	93.3:6.7
$n = 1$	−0.56	16.54	18.11	15.27	17.23	93.4:6.6
$n = 2$	1.32	19.29	20.82	18.05	20.70	93.1:6.9

[a] B_n, $TS1_n$, and C_n denote the first intermediate, the first transition state, and the second intermediate, respectively, solvated with n CO_2 molecules. The relative free energies are calculated relative to corresponding reactants in eqs 1−3. Distribution of products in the investigated reaction.

We suppose that, under the enhanced pressure of CO_2, this complex is solvated with molecules of carbon dioxide. Among different procedures to describe solvent effects at the quantum level, the use of discrete carbon dioxide molecules is selected.

MICROSOLVATED MODEL

A discrete CO_2 molecule is added to B_0 so that it is placed next to potassium (eq 2). The so-obtained structure is fully optimized without any movement restriction. Then, an additional molecule of carbon dioxide is included over the previous structure and optimized following the same procedure (eq 3). These CO_2 molecules are analogous to "normal" carbon dioxide used in the experiments of Kosugi et al. The structures containing two CO_2 moieties (intermediate B_1) and three CO_2 moieties (intermediate B_2) are presented in Figure 3. In these structures, the marked carbon atom (C7) is still analogous to the labeled carbon-13. The relative free energies of B_ns ($n = 0-2$) are given in Table 1. Our attempts to optimize structures where $n > 2$ were not successful.

Table 1 shows that the reaction 1 proceeds with the stabilization of the system. This is in accord with the experimental finding that the potassium phenoxide−carbon dioxide complex is stable at room temperature under the reduced pressure of CO_2 and confirms that the structure of the complex used for NMR and IR measurements corresponds to that of B_0. The reaction 2 is slightly exothermic, whereas the reaction 3 is slightly endothermic. Taking into account that the Kolbe−Schmitt reaction requires the conditions of high temperature and pressure to produce hydroxybenzoic acids, one can expect that the reactions 2 and 3 are likely to occur under these conditions.

The application of the natural bond orbital (NBO) analysis to B_0, B_1, and B_2 shows that their geometries are very similar. Hybridization of s and p orbitals for C7 and O8 is very small in all species (20% s and 80% p). The predominant p character of the C7 and O8 atoms with little s character indicates that these C−O bonds are weak. The lengths of the C7−O8 bonds of 1.635 Å in B_0, 1.596 Å in B_1, and 1.597 Å in B_2 are in accord with the NBO analysis. A consequence of the formation of these weak bonds is that the C7−O9 and C7−O10 bonds in B_ns are longer than those in carbon dioxide. In addition, the NBO analysis of B_0 and the solvated intermediates reveals that there is a double bond between C7 and O10, whereas the C7−O9 is a single bond in all species.

The consequence of the formation of the weak K-O11 bond in B_1 and K-O11 and K-O14 bonds in B_2 is that in both solvated intermediates the K-O9 and K-O8 bonds are somewhat longer, whereas the O8−C7 bond is shorter. In addition, the marked carbon atom is bonded to the phenolic oxygen (O8) in both B_0 and the solvated intermediates. On the basis of these facts one can suppose that the "normal" carbon dioxide in B_1 and B_2 is more flexible than the marked carbon dioxide in B_0, B_1, and B_2, so that it can easily take a suitable position to perform an electrophilic attack on the benzene ring. This assumption is supported by an analysis of HOMOs and LUMOs of B_1 and B_2. As an illustration, the HOMO and LUMO of B_1 are presented in Figure 4.

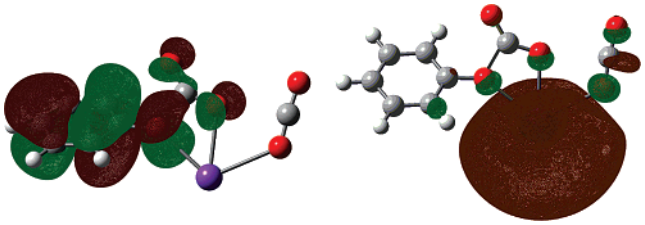

Figure 4. HOMO (left) and LUMO (right) of the potassium phenoxide−carbon dioxide complex solvated with one molecule of carbon dioxide.

The HOMO of B_1 is delocalized over many atoms, but the greatest contribution to the HOMO comes from the ortho and para carbons of the benzene ring. The LUMO is also delocalized over several atoms. As one can expect, the greatest contribution to the LUMO comes from potassium. An interesting feature of the LUMO is that it embraces the atoms of "normal" carbon dioxide, whereas the marked carbon atom does not contribute to the LUMO. This undoubtedly indicates to the site in the molecule which will perform an electrophilic attack.

Our calculations reveal that an electrophilic attack of C12 in B_1 to the ortho and para positions of the benzene ring leads to the formation of the intermediates oC_1 and pC_1 via the transition states $oTS1_1$ and $pTS1_1$, respectively (eq 5). Similarly, an electrophilic attack of C15 in B_2 to the ortho and para positions of the benzene ring leads to the formation of the intermediates oC_2 and pC_2 via the transition states $oTS1_2$ and $pTS1_2$, respectively (eq 6). The four transition states are also verified by the intrinsic reaction coordinate (IRC) calculations. The optimized geometries of the transition states are presented in Figure 5. The relative free energies for the relevant species are given in Table 1. To compare the results for models $n = 1$ and $n = 2$ to the results for model $n = 0$, the relative free energies for $n = 0$[12] are also given in Table 1.

According to the Curtin-Hammond principle, the distribution of products is determined with the difference of free energies of the ortho and para transition states. For this reason, the free energy differences between the ortho and para transition states for the conversions of B_ns are calculated. The resulting ratios between the concentrations of the ortho and para products are given in Table 1. All three ratios are mutually very similar and in agreement with the experimental results on the carboxylation reaction of potassium phenoxide.[3]

The experiments on the carboxylation reaction of different alkali metal phenoxides showed that the yield of the reaction under low pressure of CO_2 was very low and that the carboxylation reaction was competitive with the reverse reaction which led to the reactants.[3,4] On the other hand, the

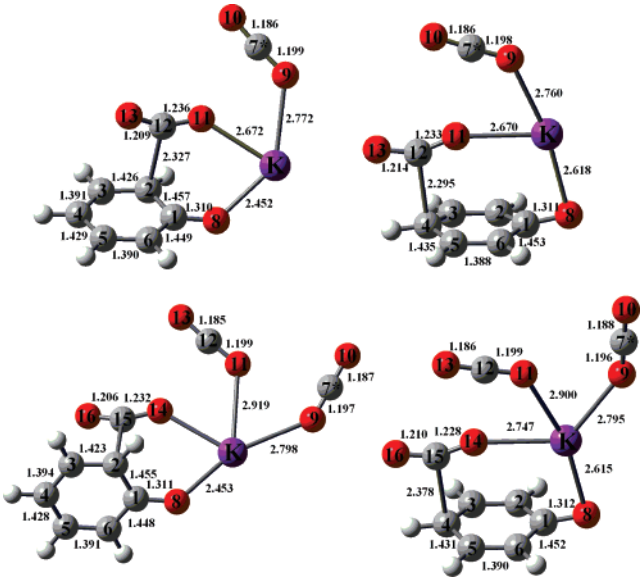

Figure 5. Optimized geometries of transition states for conversions of the potassium phenoxide−carbon dioxide complex solvated with one CO_2 molecule ($oTS1_1$ - top left and $pTS1_1$ - top right) and two CO_2 molecules ($oTS1_2$ - bottom left and $pTS1_2$ - bottom right). Distances are given in Å.

yield of the Kolbe−Schmitt reaction increased with increasing pressure.[3,4] These facts are in accord with our assumption that our model where $n = 0$ describes the conditions of low pressure of CO_2, whereas the models where $n = 1$ and 2 describe the conditions of enhanced pressure. Since the relative free energies of $oTS1_n$ and $pTS1_n$ are higher than the relative free energies of the corresponding reactants (Table 1), a reverse reaction of the conversion of B_n to the reactants can be considered. Under the reduced pressure B_0 can undergo a reverse reaction yielding PhOK and CO_2. Under the increased pressure of CO_2 the equilibrium in the reactions 2 and 3 is shifted to the right side, i.e., to the formation of the products.

Since $oTS1_n$ and $pTS1_n$ are late transition states, their structures are similar to those of the intermediates oC_n and pC_n, respectively. Since the properties of the intermediates oC_0 and pC_0 have been presented in our previous paper,[12] we will focus on the solvated intermediates (i.e., $n = 1$ and 2). The C2−C12 distance of 1.693 Å in oC_1, the C4−C12 distance of 1.721 Å in pC_1, the C2−C15 distance of 1.676 Å in oC_2, and the C4−C15 distance of 1.703 Å in pC_2 reveal the formation of new weak C−C bonds. The distance between the marked carbon (C7) and the phenolic oxygen (O8) of 5.253 Å in oC_1, 6.069 Å in pC_1, 6.301 Å in oC_2, and 6.319 Å in pC_2 shows that the O8−C7 bond is broken in the intermediates oC_n and pC_n, $n = 1$ and 2. This indicates that the intermediates oC_n and pC_n, $n = 1$ and 2, are now solvated with one or two molecules of carbon dioxide, where the marked CO_2 acts as a solvent molecule. In other words, the marked and "normal" CO_2 moieties exchanged their roles in the course of the Kolbe−Schmitt reaction.

CONCLUSIONS

Our computations furnish ambiguous support for the existence of the KOPh−CO_2 complex as an intermediate in the first stage of the carboxylation reaction of potassium phenoxide and negate the mechanism of a direct carboxylation of the benzene ring. Our investigation is in good agreement with the labeled experiments of Kosugi et al. Under the reduced pressure of carbon dioxide (0.1 MPa) the complex is not solvated with the CO_2 molecules. Its NMR and IR spectra match the computed spectra of the KOPh−CO_2 complex. Under the conditions of the Kolbe−Schmitt reaction (high pressure and temperature) the carbon-13 labeled complex is bombarded by the molecules of "normal" carbon dioxide. Carbon dioxide behaves as a solvent, and a molecule of the KOPh−CO_2 complex becomes solvated with one or two molecules of "normal" carbon dioxide. Now, the intermediate complex contains two or three CO_2 moieties, and one of them will perform an electrophilic attack. Since the carbons of the added CO_2 moieties are more flexibly bonded than the carbon-13, they can easily take a suitable position to perform an electrophilic attack on the benzene ring in both ortho and para positions. The new ortho and para intermediates are formed. These intermediates are also solvated with one or two molecules of carbon dioxide. In both cases the $^{13}CO_2$ acts as a solvent molecule. In this way a thorough mixing of $^{13}CO_2$ and "normal" CO_2 is achieved, and, as a consequence, the products of the Kolbe−Schmitt reaction contain $^{13}CO_2$ by natural abundance.

ACKNOWLEDGMENT

This work is supported by the Ministry of Science and Environment of Serbia, project no. 142025.

Supporting Information Available: *xyz*-coordinates for all computed species: B_0, B_1, B_2, $oTS1_1$, $pTS1_1$, $oTS1_2$, $pTS1_2$, oC_1, pC_1, oC_2, and pC_2. This material is available free of charge via the Internet at http://pubs.acs.org.

REFERENCES AND NOTES

(1) Kolbe, H. On the synthesis of salicylic acid. *Liebigs Ann.* **1860**, *113*, 125−127.
(2) Schmitt, R. Contribution to Kolbe's synthesis of salicylic acid. *J. Prakt. Chem.* **1885**, *31*, 397.
(3) Lindsey, A. S.; Jeskey, H. The Kolbe−Schmitt Reaction. *Chem. Rev.* **1957**, 583−620.
(4) Kosugi, Y.; Imaoka, Y.; Gotoh, F.; Rahim, M. A.; Matsui, Y.; Sakanishi, K. Carboxylation of Alkali Metal Phenoxides with Carbon Dioxide. *Org. Biomol. Chem.* **2003**, *1*, 817−821.
(5) Daives, I. A. On the formation and decomposition of sodium salicylate. *Z. Phys. Chem.* **1928**, *134*, 57−86.
(6) Ayres, D. C. *Carbanions in synthesis*; Oldbourne Press: London, United Kingdom, 1966; pp 168−173.
(7) Hales, J. L.; Jones, J. I.; Lindsey, A. S. Mechanism of the Kolbe−Schmitt reaction. I. Infrared studies. *J. Am. Chem. Soc. Abstracts* **1954**, 3145−3151.
(8) Kunert, M.; Dinjus, E.; Nauck, M.; Sieler, J. Structure and Reactivity of Sodium Phenoxide − Following the Course of the Kolbe−Schmitt Reaction. *Chem. Ber./Recueil* **1997**, *130*, 1461−1465.
(9) Stanescu, I.; Gupta, R. R.; Achenie, L. E. K. An in-silico Study of Solvent Effects on the Kolbe−Schmitt Reaction Using a DFT Method. *Mol. Simul.* **2006**, *32*, 279−290.
(10) Stanescu, I.; Achenie, L. E. K. A theoretical study of solvent effects on Kolbe−Schmitt reaction kinetics. *Chem. Eng. Sci.* **2006**, *61*, 6199−6212.
(11) Marković, Z.; Engelbrecht, J. P.; Marković, S. Theoretical Study of the Kolbe−Schmitt Reaction Mechanism. *Z. Naturforsch., A: Phys. Sci.* **2002**, *57a*, 812−818.
(12) Marković, Z.; Marković, S. Influence of Alkali Metal Cations upon the Kolbe−Schmitt Reaction Mechanism. *J. Chem. Inf. Model.* **2006**, *46*, 1957−1964.
(13) Note: The Lindsey-Jeskey citation given in refs 11 and 12 is incorrect. The correct citation is the one given in ref 3 of the current paper.
(14) Marković, S.; Marković, Z.; Begović, N.; Manojlović, N. Mechanism of the Kolbe−Schmitt Reaction with Lithium and Sodium Phenoxides. *Russ. J. Phys. Chem.* **2007**, *81*, 1−6.

(15) Lobry de Bruyn, C. A.; Tijmstra, S. Mechanism of the synthesis of salicylic acid. *Recl. Trav. Chim.* **1904**, *23*, 385−393.
(16) Johnson, J. R. Abnormal reactions of benzylmagnesium chloride. II. The mechanism of the o-tolyl rearrangement. *J. Am. Chem. Soc.* **1933**, *55*, 3029−3032.
(17) Becke, A. D. Density-functional exchange-energy approximation with correct asymptotic behavior. *Phys. Rev. A* **1988**, 3098−3100.
(18) Lee, C.; Yang, W.; Parr R. G. Development of the Colle-Salvetti correlation-energy formula into a functional of the electron density. *Phys. Rev. B* **1988**, 785−789.
(19) Becke, A. D. Density-functional thermochemistry. II. The role of exact exchange. *J. Chem. Phys.* **1993**, *98*, 5648−5652.
(20) Frisch, M. J.; Trucks, G. W.; Schlegel, H. B.; Scuseria, G. E.; Robb, M. A.; Cheeseman, J. R.; Zakrzewski, V. G.; Montgomery, J. A., Jr.; Stratmann, R. E.; Burant, J. C.; Dapprich, S.; Millam, J. M.; Daniels, A. D.; Kudin, K. N.; Strain, M. C.; Farkas, O.; Tomasi, J.; Barone, V.; Cossi, M.; Cammi, R.; Mennucci, B.; Pomelli, C.; Adamo, C.; Clifford, S.; Ochterski, J.; Petersson, G. A.; Ayala, P. Y.; Cui, Q.; Morokuma, K.; Malick, A. D.; Rabuck, K. D.; Raghavachari, K.; Foresman, J. B.; Cioslowski, J.; Ortiz, J. V.; Baboul, A. G.; Stefanov, B. B.; Liu, G.; Liashenko, A.; Piskorz, P.; Komaromi, I.; Gomperts, R.; Martin, R. L.; Fox, D. J.; Keith, T.; Al-Laham, M. A.; Peng, C. Y.; Nanayakkara, A.; Challacombe, M.; Gill, P. M. W.; Johnson, B.; Chen, W.; Wong, M. W.; Andres, J. L.; Gonzalez, C.; Head-Gordon, M.; Replogle, E. S.; Pople. J. A. *Gaussian 98, Revision A.9*; Gaussian, Inc.: Pittsburgh, PA, 1998.
(21) *Chemical Applications of Density Functional Chemistry*; Laird, A., Ross, R. B., Zeigler, T., Eds.; American Chemical Society: Washington, DC, 1996.
(22) Hay, P. J.; Wadt, W. R. Ab initio effective core potentials for molecular calculations. Potentials for the transition metal atoms Sc to Hg. *J. Chem. Phys.* **1985**, *82*, 270−283.
(23) Wadt, W. R.; Hay, P. J. *Ab initio* effective core potentials for molecular calculations. Potentials for main group elements Na to Bi. *J. Chem. Phys.* **1985**, *82*, 284−298.
(24) Hay, P. J.; Wadt, W. R. *Ab initio* effective core potentials for molecular calculations. Potentials for K to Au including the outermost core orbitals. *J. Chem. Phys.* **1985**, *82*, 299−310.
(25) Dunning, T. H., Jr.; Hay, P. J. *Modern Theoretical Chemistry;* Schaefer, H. F., Ed.; Plenum: New York, 1976; Vol. 3.
(26) Foster, J. P.; Weinhold, F. Natural hybrid orbitals. *J. Am. Chem. Soc.* **1980**, *102*, 7211−7218.
(27) The Computational Chemistry Comparison and Benchmark Database of the National Institute of Standards and Technology. http://srdata.nist.gov/cccbdb/vibscale.asp (accessed Apr 6, 2007).

CI700068B